

Piezoelectric $\text{KCo}[\text{Au}(\text{CN})_2]_3$: Room temperature crystal structure of a cobalthardened gold electrodeposition process component

S. C. Abrahams, J. L. Bernstein, R. Liminga, and E. T. Eisenmann

Citation: *The Journal of Chemical Physics* **73**, 4585 (1980); doi: 10.1063/1.440697

View online: <http://dx.doi.org/10.1063/1.440697>

View Table of Contents: <http://scitation.aip.org/content/aip/journal/jcp/73/9?ver=pdfcov>

Published by the AIP Publishing

Articles you may be interested in

[Large-strain-induced magnetic properties of Co electrodeposited on nanoporous Au](#)

J. Appl. Phys. **109**, 084315 (2011); 10.1063/1.3575327

[Microstructure of \$\text{Co}/\text{X}\$ \(\$\text{X} = \text{Cu}, \text{Ag}, \text{Au}\$ \) epitaxial thin films grown on \$\text{Al}_2\text{O}_3\$ \(0001\) substrates](#)

J. Appl. Phys. **101**, 09D122 (2007); 10.1063/1.2712956

[Co–Au core-shell nanocrystals formed by sequential ion implantation into \$\text{SiO}_2\$](#)

Appl. Phys. Lett. **89**, 153118 (2006); 10.1063/1.2360891

[Electrodeposition of nanoscale magnetic structures](#)

Appl. Phys. Lett. **73**, 3279 (1998); 10.1063/1.122744

[Effect of Co, Pt, and Au additions on the stability and epitaxy of \$\text{NiSi}_2\$ films on \(111\)Si](#)

J. Appl. Phys. **84**, 2583 (1998); 10.1063/1.368611



Piezoelectric $\text{KCo}[\text{Au}(\text{CN})_2]_3$: Room temperature crystal structure of a cobalt-hardened gold electrodeposition process component

S. C. Abrahams, J. L. Bernstein, and R. Liminga^{a)}

Bell Laboratories, Murray Hill, New Jersey 07974

E. T. Eisenmann

Bell Laboratories, Columbus, Ohio 43213

(Received 24 June 1980; accepted 21 July 1980)

Potassium cobaltous cyanoaurate(I), $\text{KCo}[\text{Au}(\text{CN})_2]_3$, a new piezoelectric material that is also a component in the electrodeposition process for cobalt-hardened gold, crystallizes in the trigonal system with space group $P312$ and one formula in the unit cell. The lattice constants at 298 K are $a = 6.82802 \pm 0.00005$, $c = 7.80807 \pm 0.00009$ Å ($\lambda_{\text{CuK}\alpha_1} = 1.540598$ Å). The integrated intensities of most reflections within a sextant of reciprocal space having radius $(\sin \theta)/\lambda \leq 1.15$ Å⁻¹ were measured diffractometrically, resulting in 1130 independent nonzero structure factors. The crystal structure was solved by use of Patterson and Fourier series and refined by the method of least squares, with final agreement factor $R = 0.0578$. The $\text{Au}(\text{CN})_2^-$ ion is close to linear, with Au–C distance of 1.994 ± 0.011 Å, C–N = 1.147 ± 0.014 Å, and C–Au–C angle of $178.2 \pm 1.7^\circ$. The Co^{2+} ion occupies an octahedral environment, with six equal Co–N distances of 2.124 ± 0.010 Å. The K^+ ion is 12-coordinated with six N atoms at 2.950 ± 0.022 Å and six C atoms at 3.215 ± 0.020 Å. A site with similar environment, but slightly shorter contacts, remains vacant. The piezoelectric d_{22} coefficient is about 5.8×10^{-12} CN⁻¹. Possible roles for $\text{KCo}[\text{Au}(\text{CN})_2]_3$ in the hard-gold electrodeposition process are considered.

INTRODUCTION

Gold that is harder than 120 kg mm^{-2} may be electrodeposited from acidic cyanoaurate(I) ions at high overvoltage.^{1,2} Such deposits represent an important class of surface finishes in the electronics industry for separable connectors and dry-reed sealed contacts.^{3,4} In a typical hard-gold deposition process, cobalt or nickel salts are added to a citrate- or phosphate-buffered solution of potassium cyanoaurate which thereby modifies the pre-chemical adsorption of gold cyanide at the electrode surface.^{5,6} The result of this addition is an increase in the activation energy of the charge transfer step,² leading to a small but significant deviation from the face-centered-cubic gold structure in the deposit,⁷ a fine grain size,⁸ and inclusion of nonmetallic impurities.^{9,10}

The mechanism by which nonmetals are codeposited in hard gold has not been established. In the case of cobalt-hardened gold, evidence has been reported that $\text{K}_3\text{Co}(\text{CN})_6$ and other cyanocobaltates account for a major proportion of light element contaminants.¹¹ It was previously shown¹² that the properties of some cyanoaurate complexes of cobalt may be correlated with the deposition characteristics of cobalt-hardened gold. Electroreduction of gold may be preceded by chemisorption of a cobalt cyanoaurate complex and followed by rearrangement to yield cyanocobaltate.

The present paper reports the crystal structure of one of the cobalt cyanoaurate complexes, which is incidentally found to be a new piezoelectric material.

EXPERIMENTAL

$\text{KCo}[\text{Au}(\text{CN})_2]_3$ precipitates from concentrated solutions of $\text{KAu}(\text{CN})_2$ and an added cobalt(II) salt.¹² Recrystallization from water yields various $\text{Co}[\text{Au}(\text{CN})_2]_2$ hydrates. Moderate-red (No. 15)¹³ hexagonal prisms with maximum dimensions less than 1 mm are obtained by digesting the precipitate for several days at 373 K in two-molar KCl. The crystals often contain small cracks which cause split diffraction spots as seen on x-ray film. It was not possible to grind a good sphere from one of the small crystals, the usual shape being slightly ellipsoidal. The best sphere, with average diameter¹⁴ of $0.179(11)$ mm, included a small misoriented volume that produced weak satellite reflections, for some crystal orientations, close to principal reciprocal lattice points. Satisfactory absorption corrections to integrated intensity measurements made on a crystal with natural faces were not possible. The error in one set of 1607 independent structure factors of this kind was such that least-squares refinement, using the best model (see below), terminated with a value of R no smaller than 0.14 .

Integrated intensity measurements were made using an Enraf-Nonius CAD-4 diffractometer controlled by a PDP 11/40-8e minicomputer.¹⁵ An ω - 2θ scan having angular range of $0.60^\circ + 0.35^\circ \tan \theta$ was used, with graphite-monochromatized $\text{MoK}\alpha$ radiation. All reflections with $0 \leq h \leq 14$, $0 \leq k \leq 14$, $-15 \leq l \leq 15$, and $(\sin \theta)/\lambda \leq 1.15$ Å⁻¹ were measured. The maximum time spent on a reflection was 120 s: backgrounds were taken by extending the scan 25% on each side. Three standard reflections measured hourly decreased steadily by an average of about 14% in the course of the experiment. A third-degree polynomial scaling function of exposure

^{a)}Permanent address: Institute of Chemistry, University of Uppsala, Box 531, S-75121, Uppsala, Sweden.

time, taken as the average of the functions for each individual standard, was applied to all reflections. A total of 3417 reflections were measured and corrected for Lorentz, polarization, and absorption¹⁶ effects (maximum and minimum transmission factors, 8.8 and 2.2%).

Standard deviations were given by the expression $\sigma^2 F^2_{\text{meas}} = V_1 + V_2$,¹⁷ where the variance V_1 is the sum of the variance due to counting statistics plus the term $30 \times 10^{-4} (F_{\text{meas}})^4$, and V_2 is the larger of that given by the deviation among equivalent members of a form and the term $278 \times 10^{-4} (F_{\text{meas}})^4$. A total of 1157 independent reflections had $F^2_{\text{meas}} > 3\sigma F^2_{\text{meas}}$. The remainder were omitted as unobserved from further analysis. An additional 14 reflections at the threshold value were later removed. Several intensity profiles had very unequal backgrounds, possibly caused by the satellite reflections. The 13 reflections with most unequal backgrounds were also omitted from the final set of F_{meas} which are given with the corresponding σF_{meas} , on the absolute scale, in Ref. 18.

CRYSTAL DATA

$\text{KCo}[\text{Au}(\text{CN})_2]_3$ has formula weight (fw) = 845.044. The trigonal unit cell has lattice constants $a = 6.82802(5)$, $c = 7.80807(9)$ Å at 298 K, as measured with $\text{CuK}\alpha_1 = 1.540598$ Å on a modified¹⁹ version of Bond's precision lattice constant diffractometer.²⁰ The usual accuracy of these measurements was reduced by the broadened 001 high-angle reflections. Lattice constants obtained by least-squares refinement, using 44 values of θ measured from a powder photograph recorded with a Guinier-Hägg XDC-700 focusing camera with $\text{CuK}\alpha_1$ radiation and using $\text{Si}(a = 5.431065)$ Å as an internal standard, are $a = 6.8277(7)$, $c = 7.8104(11)$ Å. The unit cell volume is 315.26 Å³. $D_m = 4.48(6)$ g cm⁻³, $D_x = 4.451$ g cm⁻³ for 1 fw/unit cell. The absorption coefficient²¹ for $\text{MoK}\alpha$ radiation is 36.22 mm⁻¹ and, for the sphere used, $\mu R = 3.242$. $F(000) = 361e$.

Precession and Weissenberg photographs indicated the Laue symmetry to be $6/mmm$, with no systematic absences among the reflections. The crystals are piezoelectric (see section following, also that on the piezoelectric d_{22} coefficient), hence noncentrosymmetric. Possible hexagonal space groups are $P\bar{6}m2$, $P6mm$, $P622$, or $P6$. There is also the possibility that the crystals are trigonal, with strong hexagonal pseudosymmetry caused by the metal atom contributions. Possible trigonal space groups are $P3$, $P312$, $P321$, $P3m1$, and $P31m$. Minor differences in the structure factors of reflections that would be equivalent for hexagonal symmetry were suggestive of trigonal symmetry, but were not conclusive due to the possibility of inadequate correction for the high absorption.

SOLUTION AND REFINEMENT OF THE STRUCTURE

A Patterson function was calculated using the FOUR program,²² assuming trigonal symmetry, and interpreted in terms of the lowest applicable symmetry with space group $P3$. The gold atom was thereupon found to be very close to the special position $0\frac{1}{2}0$, the cobalt atom

TABLE I. Structural refinement indicators for $\text{KCo}[\text{Au}(\text{CN})_2]_3$.^a

Parameters varied ^b	Number of variables ^c	R	wR	S
xyz, B	12	0.1368	0.1867	1.765
yxz, B	13	0.1344	0.1822	1.723
xyz, β_{ij} (Metals) $B(C, N)$	18	0.0627	0.0985	0.934
yxz, β_{ij} (Metals) $B(C, N)$	18	0.0583	0.0875	0.833
xyz, β_{ij} (All atoms)	28	0.0617	0.0960	0.917
yxz, β_{ij} (All atoms)	28	0.0578	0.0865	0.823

^aSee Ref. 17 for definitions of R , wR , and S .

^bA single scale factor is varied, with no correction necessary for extinction.

^cFor 1130 independent F_{meas} , given in Ref. 18.

close to $00\frac{1}{2}$. Least-squares refinement in which the only variables were the scale factor and the z coordinate for Co gave phase angles that were used in a difference Fourier synthesis to reveal the location of the K atom at $\frac{2}{3}, \frac{1}{3}, z$ with z close to $\frac{1}{2}$. Initial coordinates for the two independent CN^- ions also found in this synthesis were confirmed by further least-squares refinement. Atomic scattering factors for neutral atoms were taken from the *International Tables for X-Ray Crystallography*,²¹ as were corrections for anomalous dispersion. The calculations were made on the Honeywell 6080 computer with the ORFLS-3 program.²³ Refinement was continued with a model in which the metal atoms were allowed to vibrate anisotropically, the two CN^- ions isotropically. No significant density remained in the corresponding difference Fourier series, nor did the refined z coordinates for Co or K differ from $\frac{1}{2}$.

Piezoelectric measurements, however, showed that the d_{33} coefficient is not detectable for the small crystals available, but that d_{22} is moderately strong. No pyroelectric signal was detected, either along or normal to the c axis. Assuming the undetectable coefficients have zero magnitude, the only space groups compatible with these observations are $P312$, $P321$, and $P\bar{6}m2$. The atomic coordinates of the two independent CN^- ions could be given in $P312$ by placing a single independent CN^- ion in the sixfold position and keeping the metal atom positions unchanged, but not in the two other choices of space group without assuming a disordered model. Refinement converged smoothly in $P312$, with Au in position $3j$ at $2\bar{x}, \bar{x}, 0$. The refinement indicators are given in Table I, the final atomic coordinates in Table II, and the anisotropic temperature coefficients in Table III. The fit between the F_{meas} and F_{calc} for the final model, as listed in Ref. 18, is illustrated by the δR normal probability plot²⁴ shown in Fig. 1. In the absence of systematic error, the plot would be linear with zero intercept. Apart from some deviations in the extrema the plot in Fig. 1 is close to linear, with zero intercept. The slope of 0.82 indicates the σF_{meas} are overestimated by about 22%; the linearity indicates a lack of serious systematic error either in the model or in the measurements.

The possibility of disorder in the CN^- ion arrange-

TABLE II. Atomic position coordinates in $\text{KCo}[\text{Au}(\text{CN})_2]_3$ at 298 K.^a

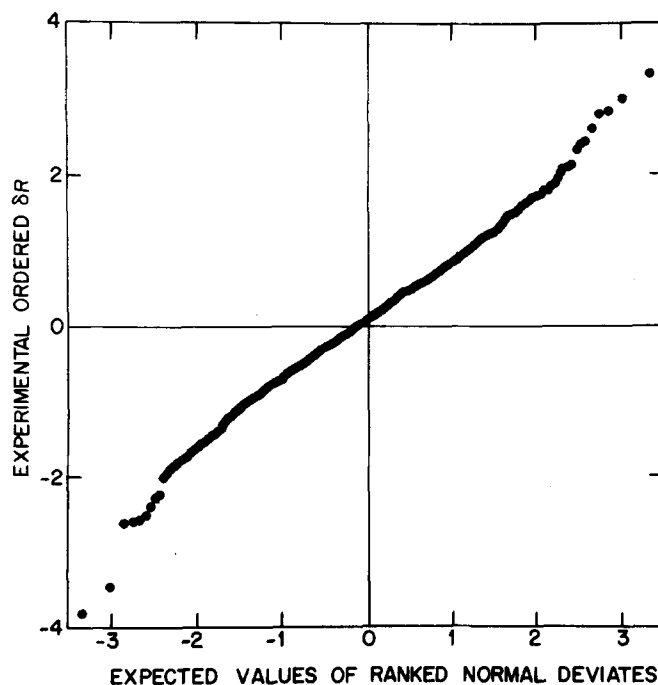
Atom	<i>x</i>	<i>y</i>	<i>z</i>
K	0.3333	0.6667	0.5000
Co	0	0	0.5000
Au	0.9918(3)	0.4959	0
C	0.987(5)	0.650(3)	0.2149(13)
N	0.995(4)	0.752(2)	0.3341(13)

^aCoordinates correspond to the *yxz* model of Table I: values without parentheses are constants, with K in position 1*d*, Co in 1*b*, and Au in 3*j* of space group *P*312.

ment, as required by the alternative choice of space groups, was investigated: models with *wR* less than 0.158 could not be obtained, hence they were rejected. Also investigated was the possibility in space group *P*312 that the carbon and nitrogen atoms had been inadvertently interposed. Least-squares refinement in which the two sets of atomic scattering factors were interchanged led to the indicators $R=0.0594$, $wR=0.0891$, $S=0.848$. The hypothesis that the identities of C and N in Table II are interchanged can be tested by use of the Hamilton ratio²⁵ $R_{15, 1102, 0.005} = 1.004$. The experimental ratio is given by $0.0891/0.0865=1.030$ (see Table I), hence the hypothesis can be rejected at the half-percent significance level.

AMPLITUDES OF VIBRATION

It is also possible to test the hypotheses that (a) the atomic vibrations of all atoms in $\text{KCo}[\text{Au}(\text{CN})_2]_3$ are isotropic, and (b) the metal atoms only vibrate anisotropically, on the basis of the refinement indicators listed in Table I. For hypothesis (a), the experimental ratio $wR(\text{isotropic})/wR(\text{anisotropic})=2.106$, whereas the Hamilton ratio²⁵ $R_{15, 1102, 0.005} = 1.015$, hence it may be confidently rejected at the half-percent significance level. For hypothesis (b), the experimental ratio from Table I is 1.012, the Hamilton ratio is 1.010, hence it may also be rejected. The degree of anisotropy in the thermal vibrations is shown by the range in root-mean-square amplitudes given in Table IV. The K^+ ion vibrates rather isotropically, but both Co^{2+} and Au^+ are strongly anisotropic, with a ratio for the major/minor principal ellipsoid axes of 1.78 for Au^+ . The CN^- ion is also strongly anisotropic in vibrational amplitude, the

FIG. 1. Normal probability plot of 1130 δR statistics.²⁵

axial ratio for the carbon atom linked to Au being less than that of the nitrogen atom (see Table IV). The absolute magnitudes of the ellipsoids of vibration are comparable to those found in many inorganic salts, such as $\text{Ba}(\text{NO}_2)_2 \cdot \text{H}_2\text{O}$ ²⁶ and $\text{Ni}(\text{IO}_3)_2 \cdot 2\text{H}_2\text{O}$.²⁷

ABSOLUTE CONFIGURATION

Anomalous scattering by the metal atoms in $\text{KCo}[\text{Au}(\text{CN})_2]_3$ results in the condition, for space group *P*312, that $F(hk \cdot l) \neq F(kh \cdot l)$. Hence, for the right-handed set of Miller indices in Ref. 18, two chiralities for the atomic arrangement are to be considered, one with coordinates *xyz*, the other with coordinates *yxz*. The hypothesis that the structure amplitudes calculated with *xyz* coordinates fit the measured amplitudes in Ref. 18 better than those calculated with *yxz* coordinates is readily tested, for $wR(\text{xyz})/wR(\text{yxz})=1.110$ whereas the theoretical value is 1.004 (see above). The hypothesis may hence be rejected with confidence at the half-percent significance level. The atomic position coordinates in Table II correspond to the *yxz* chirality of Table I.

TABLE III. Anisotropic temperature coefficients for $\text{KCo}[\text{Au}(\text{CN})_2]_3$ at 298 K.^a

Atom	β_{11}	β_{22}	β_{33}	β_{12}	β_{13}	β_{23}
K	191(16)	191	121(12)	96	0	0
Co	121(5)	121	34(2)	60	0	0
Au	197(3)	128(3)	57.9(6)	64	0	-29.4(7)
C	187(45)	191(50)	57(10)	106(50)	-20(26)	-28(18)
N	220(36)	109(33)	79(11)	54(3)	76(27)	7(16)

^aBased on the exponential expression $-(\beta_{11}h^2 + \beta_{22}k^2 + \beta_{33}l^2 + 2\beta_{12}hk + 2\beta_{13}hl + 2\beta_{23}kl)$. Values of β_{ij} are $\times 10^4$. See footnote to Table II.

TABLE IV. Root-mean-square amplitudes of thermal vibration along the principal ellipsoid axes in $\text{KCo}[\text{Au}(\text{CN})_2]_3$ at 298 K.

Atom	1	2	3
K	0.184(10)	0.184	0.194(10)
Co	0.102(4)	0.146(4)	0.146
Au	0.112(1)	0.165(1)	0.199(2)
C	0.123(14)	0.172(25)	0.193(27)
N	0.112(19)	0.141(19)	0.240(22)

TABLE V. Interatomic distances and angles in $\text{KCo}[\text{Au}(\text{CN})_2]_3$ at 298 K.^a

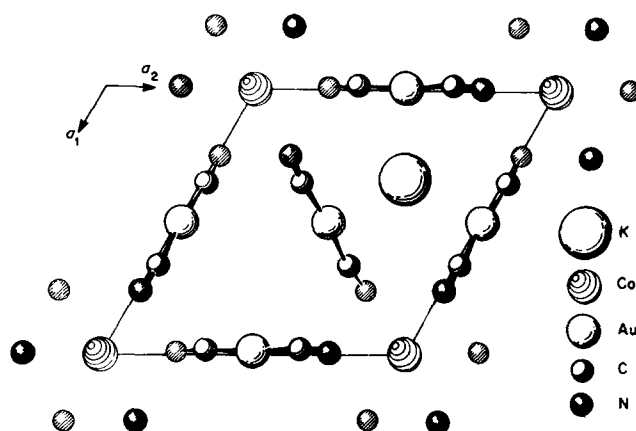
Au—C	1.994(11) Å × 2	C—N	1.147(14) Å
Co—N	2.124(10) × 6	K—N	2.950(22) × 6
Co—C	3.239(12) × 6	K—C	3.215(20) × 6
C—Au—C	178.2 ± 1.7°	Vacancy ^b —N	2.912(22) × 6
N—C—Au	175.4 ± 2.2°	Vacancy—C	3.117(20) × 6

^aThe number of equivalent distances follows the multiplication sign.

^bThe vacant site is at $\frac{2}{3}, \frac{1}{3}, \frac{1}{2}$; see text.

IONIC PACKING ARRANGEMENT

A view of the atomic arrangement in $\text{KCo}[\text{Au}(\text{CN})_2]_3$, as seen along the trigonal direction, is given in Fig. 2. The cobalt ion lies on the trigonal axes passing through the unit cell vertices with $z = \frac{1}{2}$, the potassium ion on one of the remaining two trigonal axes, also with $z = \frac{1}{2}$. The approximately linear $\text{Au}(\text{CN})_2^-$ ion (see Interatomic Distances and Angles, below) is close to and nearly parallel with the ac face. The length of the $\text{Au}(\text{CN})_2^-$ ion is inclined at an angle of about 57° to the a axis, with the Au atom at $z = 0$. The operation of the trigonal axes produces similar but different environments about the two axes at $\frac{1}{3}, \frac{2}{3}, z$ and $\frac{2}{3}, \frac{1}{3}, z$ which intersect the K^+ ion and a vacant site, respectively. The nearest neighbors surrounding the K^+ ion are somewhat more distant than those about the vacant site, as may be seen below. The possibility that the vacancy is not empty may be rejected since the maximum residual electron density at this site is less than $1e \text{ \AA}^{-3}$: further least-squares refinement of a model with half a K^+ ion placed on each of the two interior trigonal axes, at $z = \frac{1}{2}$, led to the occupancy factor

FIG. 2. Projected view of $\text{KCo}[\text{Au}(\text{CN})_2]_3$ along the trigonal direction. The ionic representation is given by the key.

of the location at $\frac{2}{3}, \frac{1}{3}, \frac{1}{2}$ becoming zero, that at $\frac{1}{3}, \frac{2}{3}, \frac{1}{2}$, i.e., the position shown in Fig. 2, becoming equivalent to one complete K^+ ion.

INTERATOMIC DISTANCES AND ANGLES

The cyanoaurate ion in $\text{KCo}[\text{Au}(\text{CN})_2]_3$ at room temperature is not space group restricted to a particular configuration. As may be seen in Table V, in which the interatomic distances and angles are calculated using ORFFE²³ from the coordinates of Table II and the lattice constants given under "Crystal Data," the $\text{Au}(\text{CN})_2^-$ ion is close to linear. A similar result has been found in other cyanoaurates, as summarized in Table VI. The linear C—Au—C group in $\text{KAu}(\text{CN})_2$ results from the location of the Au atom at an inversion center,²⁸ but neither this nor the Au—C—N angle departs significantly from linearity in any of the studies reported. The weighted mean C—N distance from the data in Table VI is 1.156(12) Å, that of Au—C is 1.989(9) Å. Infrared and Raman spectroscopic studies³² also indicate a linear $\text{Au}(\text{CN})_2^-$ ion both in solution and in the solid.

The Co^{2+} ion occupies a site with symmetry close to that of a regular octahedron, as seen in Fig. 3, with N—Co—N angles of $86.5(5)^\circ$ and $178.5(1.3)^\circ$ and six Co—N distances of 2.124(10) Å. This arrangement is in contrast to the coordination about Co^{3+} in the stable

TABLE VI. Cyanoaurate ion dimensions.

Compound	C—N (Å)	Au—C (Å)	Au—C—N (deg)	C—Au—C (deg)	Ref.
$\text{KAu}(\text{CN})_2$	1.17(20)	2.12(14)	172.8(7.5)	180	28
$\text{AuCN}(\text{CNCH}_3)$	1.15(6)	2.01(4)	175(4)	176(2)	29
	1.18(6)	1.98(5)	179(4)		
$\text{K}[\text{Au}(\text{CN})_2] \cdot \text{C}_{10}\text{H}_8\text{N}_2$	1.16(5)	1.98(4)	175(3)	176(2)	30
	1.10(5)	2.04(4)	172(3)		
$\text{AuCN}(\text{C}_6\text{H}_5)_3\text{P}$	1.25(4)	1.85(4)			31
$\text{K}[\text{Au}(\text{CN})_2\text{Cl}_2]\text{H}_2\text{O}$	1.20(18)	2.03(12)	161(7)	180	35
$\text{KCo}[\text{Au}(\text{CN})_2]_3$	1.147(14)	1.994(11)	175.4(2.2)	178.2(1.7)	This work

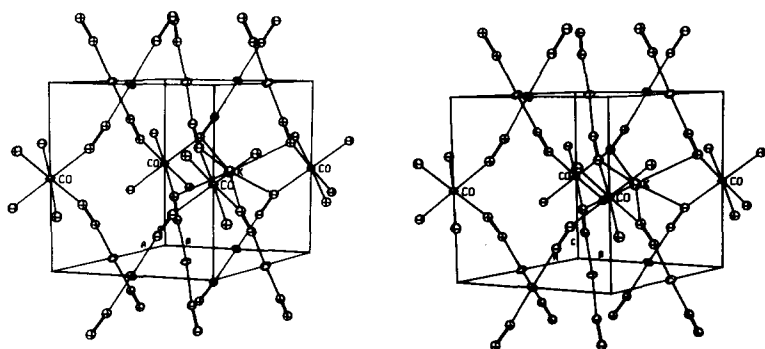


FIG. 3. Stereoscopic view of the contents of one unit cell of $\text{KCo}[\text{Au}(\text{CN})_2]_3$.

$\text{Co}(\text{CN})_6^{3-}$ ion, in which the carbon atoms are directly linked to Co, with Co–C about 1.90 Å [cf. Co–C = 1.904(5) Å in the anion of $\text{Co}(\text{III})(\text{C}_{10}\text{H}_8\text{N}_8) \cdot \text{Co}(\text{III})(\text{CN})_6 \cdot 3\text{H}_2\text{O}$].³³ The preservation of $\text{Au}(\text{CN})_2^-$ or $\text{Co}(\text{NC})_6^{4-}$ complex ions rather than the formation of $\text{Co}(\text{CN})_6^{3-}$ ions in the gold electrodeposition solution is considered to be of significance in depositing hard gold.

The K^+ ion is in close contact with six CN^- ions, see Fig. 3. Six N atoms are equidistant at 2.950(22) Å, six C atoms at 3.215(20) Å. The K–N approach slightly exceeds the normal range for six coordination, e.g., K–N = 2.70–2.83(14) Å in $\text{KAu}(\text{CN})_2$,²⁸ 2.789–2.824(12) Å in $\text{Cs}_2\text{K}[\text{Fe}(\text{CN})_6]$,³⁴ and 2.84(13) Å in $[\text{K}[\text{Au}(\text{CN})_2\text{Cl}_2] \cdot \text{H}_2\text{O}]$.³⁵ The K atom in $\text{KCo}[\text{Au}(\text{CN})_2]_3$ is 12 coordinated, hence the K^+ radius is expected to be larger than in these other materials. The environment about the vacant site at $\frac{2}{3}, \frac{1}{3}$, $\frac{1}{2}$ is very similar to that about the K^+ ion, with six nearest CN^- ions of which the N atoms are 2.912 Å and the C atoms are 3.117 Å distant. The K^+ ion is 3.942 Å from the vacant site, appreciably less than the closest K–K approach distance of 4.607 Å in the metal or that of 4.203 Å in $\text{KAu}(\text{CN})_2$. The forces causing this site to remain vacant are taken as originating in the close contacts that would otherwise result.

ROLE OF $\text{KCo}[\text{Au}(\text{CN})_2]_3$ IN THE GOLD ELECTRODEPOSITION PROCESS

Consideration of the atomic arrangement in $\text{KCo}[\text{Au}(\text{CN})_2]_3$ leads to two plausible roles for this compound in the process of electrodepositing cobalt-hardened gold. Since hard gold typically has a grain size less than 10^{-3} mm whereas soft-gold deposits contain small columnar crystals of the pure element, both roles are expected to lead to curtailment of grain growth caused by the inclusion of impurities. In the first, the octahedral configuration of CN^- ions about the Co^{2+} ion may result in the formation of $\text{Co}(\text{NC})_6^{4-}$ complexes in solution. The length, hence strength, of the six Co(II)–N contacts in $\text{KCo}[\text{Au}(\text{CN})_2]_3$ is comparable to that of the more common Co(III)–N bond length of about 1.98 Å, since the radius³⁶ of Co^{2+} is 0.10–0.14 Å greater than Co^{3+} (depending on the spin state). Adsorption of $\text{Co}(\text{NC})_6^{4-}$ ions in the cathodic surface layer would give rise to the observed coupled inclusion of cobalt, nitrogen, and carbon in the gold deposit,¹⁰ thereby reducing grain growth. It has been reported that cyanides in the form of AuCN , $\text{KAu}(\text{CN})_2$, or $\text{KAu}(\text{CN})_4$ cannot account for the observed carbon content.³⁷

The second role may be related to a postulated epitaxial overgrowth of $\text{KCo}[\text{Au}(\text{CN})_2]_3$ on surfaces of deposited gold. The Au–Au spacing in the element is 3.53 Å and in $\text{KCo}[\text{Au}(\text{CN})_2]_3$ it is 3.33 and 3.50 Å, with a trigonal arrangement of gold atoms in both. Such overgrowth would lead to curtailment in the growth of the gold surface. Further, the slight mismatch in spacing could excite the d_{22} piezoelectric coefficient, causing a polarization in the deposition plane, with consequent attraction of impurities and reduced growth of the gold particles.

Additional studies of related components in cobalt-hardened gold electrodeposition are necessary for further understanding of this complex process.

PIEZOELECTRIC d_{22} COEFFICIENT IN $\text{KCo}[\text{Au}(\text{CN})_2]_3$

A preliminary measurement of the d_{22} coefficient was made by a static method.³⁸ Opposite pairs of prism faces were coated with Engelhard's flexible silver coating. The charge produced on these faces was measured with a Keithley 610C electrometer as a calibrated tensile stress was removed. The resulting value for d_{22} was $5.8 \times 10^{-2} \text{ CN}^{-1}$.

ACKNOWLEDGMENTS

It is a pleasure to thank the Swedish Natural Science Research Council and the University of Uppsala for grants to one of us (R. L.).

- ¹H. A. Reinheimer, J. Electrochem. Soc. **121**, 490 (1974).
- ²E. T. Eisenmann, J. Electrochem. Soc. **125**, 717 (1978).
- ³R. Duva and D. G. Foulke, Plating **55**, 1056 (1968).
- ⁴M. Antler, in *Gold Plating Technology*, edited by F. H. Reid and W. Goldie (Electrochemistry Publications, Ayr, Scotland, 1974), pp. 259–294.
- ⁵J. A. Harrison and J. Thompson, J. Electroanal. Chem. **40**, 113 (1972).
- ⁶D. W. Kirk, F. R. Foulkes, and W. T. Grayton, J. Electrochem. Soc. **125**, 1436 (1978).
- ⁷E. T. Eisenmann, J. Electrochem. Soc. **127**, 1349 (1980).
- ⁸Y. Okinaka and S. Nakahara, J. Electrochem. Soc. **123**, 1284 (1976).
- ⁹G. B. Munier, Plating **56**, 1151 (1969).
- ¹⁰C. J. Raub, A. Knoedler, and J. Lendvay, Plat. Surf. Finish **63**, 35 (1976).
- ¹¹R. L. Cohen, F. B. Koch, L. N. Schoenberg, and K. W. West, J. Electrochem. Soc. **126**, 1608 (1979).
- ¹²E. T. Eisenmann, J. Electrochem. Soc. **124**, 1957 (1977).
- ¹³K. L. Kelly and D. B. Judd, Natl. Bur. Stand. Circ. **553**

- (1965) (including supplement, Standard Sample No. 2106).
- ¹⁴Error values here and elsewhere in this paper in parentheses correspond to the least significant digits in the function value.
- ¹⁵*Enraf-Nonius CAD-4 Operation Manual*, Delft, 1979.
- ¹⁶K. Weber, *Acta Crystallogr. Sect. B* **25**, 1174 (1969).
- ¹⁷S. C. Abrahams, J. L. Bernstein, and E. T. Keve, *J. Appl. Crystallogr.* **4**, 284 (1971).
- ¹⁸See AIP Document No. PAPS JCPSA-73-4585-04 for 04 pages of both Murray Hill and Uppsala measured and calculated structure factors of $\text{KCo}[\text{Au}(\text{CN})_2]_3$ at 298 K. Order by PAPS number and journal reference from American Institute of Physics, Physics Auxiliary Publication Service, 335 East 45th Street, New York, NY 10017. The price is \$1.50 for each microfiche (98 pages) or \$5.00 for photocopies of up to 30 pages with \$0.15 for each additional page over 30 pages. Airmail additional. Make checks payable to the American Institute of Physics. This material also appears in *Current Physics Microfilm*, the monthly microfilm edition of the complete set of journals published by AIP, on the frames immediately following this journal article.
- ¹⁹R. L. Barns, *Mater. Res. Bull.* **2**, 273 (1967).
- ²⁰W. L. Bond, *Acta Crystallogr.* **13**, 814 (1960).
- ²¹J. A. Ibers and W. C. Hamilton (Eds.), *International Tables for X-Ray Crystallography*, (Kynoch, Birmingham, 1974), Vol. IV.
- ²²C. J. Fritchie (unpublished), modified by L. Guggenberger and P. B. Jamieson.
- ²³W. R. Busing, K. O. Martin, and H. A. Levy, *J. Appl. Crystallogr.* **6**, 309 (1973).
- ²⁴S. C. Abrahams and E. T. Keve, *Acta Crystallogr. Sect. A* **27**, 157 (1971).
- ²⁵W. C. Hamilton, *Acta Crystallogr.* **18**, 502 (1965).
- ²⁶S. C. Abrahams, J. L. Bernstein, and R. Liminga, *J. Chem. Phys.* **72**, 5857 (1980).
- ²⁷S. C. Abrahams, J. L. Bernstein, J. B. A. A. Elemans, and G. C. Verschoor, *J. Chem. Phys.* **59**, 2007 (1973).
- ²⁸A. Rosenzweig and D. T. Cromer, *Acta Crystallogr.* **12**, 709 (1959).
- ²⁹S. Esperas, *Acta Chem. Scand. A* **30**, 527 (1976).
- ³⁰P. G. Jones, W. Clegg, and G. M. Sheldrick, *Acta Crystallogr. Sect. B* **36**, 160 (1980).
- ³¹P. L. Bellon, M. Manassero, and M. Sansoni, *Ric. Sci.* **39**, 173 (1969).
- ³²B. M. Chadwick and S. G. Frankiss, *J. Mol. Struct.* **31**, 1 (1976).
- ³³S. Sato and Y. Saito, *Acta Crystallogr. Sect. B* **31**, 2456 (1975).
- ³⁴S. R. Fletcher and T. C. Gibb, *J. Chem. Soc. Dalton* **1977**, 309.
- ³⁵C. Bertinotti and A. Bertinotti, *C. R. Acad. Sci. Paris B* **273**, 33 (1971).
- ³⁶R. D. Shannon, *Acta Crystallogr. Sect. A* **32**, 751 (1976).
- ³⁷R. L. Cohen, K. W. West, and M. Antler, *J. Electrochem. Soc.* **124**, 342 (1977).
- ³⁸IEEE Std. 176. Institute of Electrical and Electronic Engineers *Standard on Piezoelectricity*, New York (1978).